Finite Difference Formulas for Neumann Conditions on Irregularly Shaped Boundaries

Abstract: A method, based on finite element techniques, is described for obtaining finite differences for Neumann conditions on irregularly shaped boundaries. The resultant difference equations may be used in both time-dependent and -independent problems. As an example, the propagation of an elastic surface wave (Rayleigh wave) around a 90° corner is studied. The results of this simulation compare favorably with laboratory experiments.

Introduction

The finite element method for the numerical solution of partial differential equations (referred to in this paper as PDE's) has found application in many fields since its introduction in 1956 by Turner et al. [1] for airframe structure design. Most of the applications have involved elliptic PDE's, although some parabolic and hyperbolic PDE's have been solved by this method. In contrast to the older finite difference method, the finite element method offers certain advantages:

- Neumann boundary conditions, involving derivatives of the field variable, are easily applied over irregular boundaries.
- The elements may be chosen to be small in regions where the range of values of the solution is expected to be large and vice versa, thereby conserving on storage requirements and computation time.

This latter advantage is purchased at the price of adding complicated logic to the computer program.

The finite element method and the finite difference method are generally considered to be completely different approaches to the numerical solution of PDE's. However, Friedrichs and Keller [2] have demonstrated that for linear approximation functions over triangular elements whose nodes are grid points of a rectangular net, the two methods yield the same difference formulas at interior points. It is therefore possible to choose a hybrid method midway between the finite element and finite

difference methods. One starts with a rectangular grid, thereby forfeiting the second advantage, but greatly simplifying the logical design of the program. Having chosen a rectangular grid, one may immediately use the standard centered difference formulas for the interior points. Then the finite element method may be used to obtain difference formulas for the boundary points. The first advantage is thus preserved. This is of particular value if one already has a finite difference code for some problem and wishes to consider cases in which the boundaries are irregular. Furthermore, the only requirement is that the grid be rectangular. Since there is no requirement of fixed intervals between points, some flexibility in the size of the elements is possible.

Friedrichs and Keller obtained their difference formulas by a variational approach. In the next section, it will be shown how Friedrichs and Keller's piecewise linear functions with compact support (termed tent functions) may be used to obtain finite difference formulas by the standard engineering approach to the finite element method. In this and following sections it will be assumed that the reader has a knowledge of the finite element method equivalent to the material contained in the first two chapters of Ref. 3. The following section will discuss the extension of the finite element method to time-dependent problems. Finally, the results of computations, using this method, will be described for an elastic surface wave (Rayleigh wave) on a quarter space and compared with

365

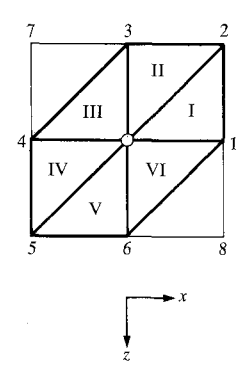


Figure 1 Hexagonal tent function centered about the grid point 0. The six sides indicated by Roman numerals are planar. The amplitude at the point 0 is one, and it is zero all around the boundary.

Table 1 Components of tent function.

Region	Function
I	1-x/h
11	1+z/k
III	1+z/k+x/h
IV	1 + x/h
V	1-z/k
VI	1-z/k-x/h

model experiments of other authors. This is an example of a problem that has defied analytic solution [4], for which a recourse to numerical solution is justified.

Difference formula derivation for finite elements

Let a rectangular grid in the x,z plane be given with the diagonals from lower left to upper right drawn in to yield a triangularization of the plane. The quantities to be calculated are the nodal displacements in a region \mathcal{R} of the plane with boundary \mathcal{R} on which Neumann conditions are given. Assume that within each triangle the displacements are a linear function of the displacements at the vertices of the triangle. If one imagines the displacements to be vertical displacements, then the plane of the triangle is shifted to a plane passing through the displaced vertices.

Next consider the planes formed by partial displacements such that the displacement at any two nodes is set equal to zero, while the displacement at the remaining node assumes its previous value. There are three such planes for each triangle. The sum of the partial displacements is the original displacement, since the sum must be linear and has the same values at three points, the vertices.

An alternate formulation is obtained using Friedrichs and Keller's tent function as shown in Fig. 1. Since our

examples will be taken from elasticity models, we follow the common procedure of choosing z positive downwards. Therefore the y axis is directed out of the page. The function is identically zero everywhere except in the six triangles numbered with Roman numerals. The central mesh point is numbered zero, and the six outside mesh points are numbered in a counterclockwise sense starting at the positive x-axis. The tent function is a continuous function made up of linear functions defined over the six triangles such that the value of every function is unity at the central mesh point and zero at the outside mesh points. Assume similar functions centered about the other mesh points. Then the three tent functions centered about the points 0, 1, and 2 and no others will have nonzero values over triangle I. Thus the displacement at a point (x,z) of the triangular element I may be written as $\sum_{i=0}^{2} \delta_{i} T_{i}(x,z)$ where δ_{i} is the displacement at the apex i and $T_i(x,z)$ is the value of the tent function about the apex i at the point (x,z).

Friedrichs and Keller used these tent functions centered on the grid points as trial functions for solving elliptic PDE's by the Ritz method. We will use them in the usual engineering procedure for deriving stiffness matrices, since the method for handling irregular boundaries is more easily seen in this way.

Following Zienkiewicz, we first obtain the B matrix which, when multiplied by the displacement vector, yields the strain components. We will assume the simplest case of transverse motion (in the y direction) so that the strain components are $\partial v/\partial x$ and $\partial v/\partial z$, where v is the transverse displacement.

In Fig. 1, let us assume that the central mesh point is at the origin, that the spacing along the x axis is h and along the z axis k. Then we may make a table of the equations for the six planes, the parts of which make up the tent function.

The calculation of strains involves taking derivatives so that only the slopes of the planes, which are not functions of x and z, are of importance. Therefore, it suffices to consider only the region about the origin. We begin by making a table of derivatives from Table 1.

The B matrix for region I will be a 2×3 matrix since it gives two strain components from the displacements of the three vertices. The strains are obtained by multiplying the value of the displacement at the origin, v_0 , by the derivatives for I in Table 2 and adding to it v_1 times the derivatives for III and v_2 times the derivatives for V. This procedure is appropriate since the part of the tent function about point 1 which covers I has the same slope as III, and that about 2 has the same slope as V. Thus the B matrix for I is

$$\begin{bmatrix} -1/h & 1/h & 0 \\ 0 & 1/k & -1/k \end{bmatrix}. \tag{1}$$

Table 2 Derivatives.

	I	П	III	IV	V	VI
$\frac{\partial}{\partial x}$ $\frac{\partial}{\partial z}$	-1/h	0 1/k	1/h 1/k	1/h 0	0 -1/k	-1/h - 1/k

Note that since the B matrix is not a function of x and z, the strain is the same everywhere in region I. This is the case only when the trial functions chosen are linear.

Next the D matrix, which gives the stress components in terms of the strain components, is required. For this case we will assume that a constant factor μ_1 times each strain component yields the stress. Hence $D = \mu_1$ times the 2×2 identity matrix. Finally, the stiffness matrix K_1 for I is $\int_1 B^T D B \, dx \, dz$, where B^T is the transpose of B, and the integration is carried out over region I. Since $B^T D B$ is constant under the above assumptions, the effect of the integration is to multiply the constant by (1/2)hk. Evaluation of this quantity yields

$$K_{1} = (1/2)hk\mu_{1} \begin{bmatrix} 1/h^{2} & -1/h^{2} & 0\\ -1/h^{2} & (1/h^{2}) + (1/k^{2}) & -1/k^{2} \\ 0 & -1/k^{2} & 1/k^{2} \end{bmatrix}.$$
 (2)

This matrix multiplied by the displacements at 0, 1, and 2 yields the forces at 0, 1, and 2 resulting from the straining of I. To find the total force at 0, the stiffness matrices for the remaining five regions must be evaluated and combined. The result is a 7×7 matrix which yields the forces at the seven grid points due to straining of the six elements. Only the force at 0 is complete, since neighboring regions will make contributions to the forces at the outside points. Therefore, we are interested only in the product of the first row of the stiffness matrix times the displacements, which yields the force at 0, F_0 . The result is:

$$\begin{split} 2F_0/hk &= \left[\left(1/h^2 \right) \left(\mu_1 + \mu_3 + \mu_4 + \mu_6 \right) \right. \\ &+ \left. \left(1/k^2 \right) \left(\mu_2 + \mu_3 + \mu_5 + \mu_6 \right) \right] v_0 \\ &- \left. \left(1/h^2 \right) \left(\mu_1 + \mu_6 \right) v_1 - \left(1/k^2 \right) \left(\mu_2 + \mu_3 \right) v_3 \\ &- \left(1/h^2 \right) \left(\mu_3 + \mu_4 \right) v_4 - \left(1/k^2 \right) \left(\mu_5 + \mu_6 \right) v_6 \,. \end{split} \tag{3}$$

If we assume that the μ 's are the same for all six triangular elements, the formula on the right is just the negative of the usual centered difference formula for the Laplacian. A difference approximation for the Laplacian is to be expected since an obvious sample of the strain and stress assumed here is the deformed membrane, which satisfies Laplace's equation.

As the next example consider plane strain. At each node there will be two horizontal components of displacement, u and w, and two horizontal components of force. The three components of strain are $\partial u/\partial x$, $\partial w/\partial z$, and

 $(\partial u/\partial z) + (\partial w/\partial x)$. The *B* matrix for a triangular element will therefore be 3×6 . The *D* matrix [5] is 3×3

$$D = \begin{bmatrix} \lambda + 2\mu & \lambda & 0 \\ \lambda & \lambda + 2\mu & 0 \\ 0 & 0 & \mu \end{bmatrix}, \tag{4}$$

where λ and μ are the Lamé constants for an isotropic medium.

Once again the stiffness matrix is calculated for each triangular element. It is now 6×6 . The stiffness matrix for all six elements is now 14×14 , of which only the first two rows are of interest. If we assume a homogeneous medium, the first row (which gives the component of force at the 0 grid point in the x direction) is

$$2\frac{F_{0x}}{hk} = \frac{2(\lambda + 2\mu)}{h^2} (2u_0 - u_1 - u_4) + \frac{2\mu}{k^2} (2u_0 - u_3 - u_6) + \frac{\lambda + \mu}{hk} (2w_0 - w_1 + w_2 - w_3 - w_4 + w_5 - w_6).$$
(5)

The appropriate differential equation [5] for F_{0x} is:

$$\frac{F_{0x}}{hk} = (\lambda + 2\mu) \frac{\partial^2 u}{\partial x^2} + \mu \frac{\partial^2 u}{\partial z^2} + (\lambda + \mu) \frac{\partial^2 w}{\partial x \partial z}.$$
 (6)

The procedure again yields the ordinary centered difference formula for the first two second derivatives. The third expression on the right of (5) is an expression for $\Delta^2 w/\Delta w \Delta z$. Normally we would expect

$$\frac{\Delta^2 w}{\Delta x \Delta z} = \frac{w_2 - w_7 - w_8 + w_5}{4hk},\tag{7}$$

where the grid points 7 and 8 are shown in Fig. 1. However, since 7 and 8 are not part of the region covered by the tent function about 0, a different expression for $\Delta^2 w/\Delta x \Delta z$ is obtained.

There is obviously some asymmetry being introduced here. Why should the points 2 and 5 be favored over the points 7 and 8, which are equally as close to 0? The tent function might just as well be drawn as in Fig. 2. If one calculates a difference formula for F_{0x} for this configuration a result similar to (5) results. Finally, if one takes the average of the two expressions for F_{0x} , the usual centered difference formula for $\Delta^2 w/\Delta x \Delta z$, (7), is obtained.

The procedure at a boundary is clear. For example, if the boundary \mathcal{B} is defined by z = constant, only half of the tent function will lie in the region \mathcal{B} . This is illustrated in Fig. 3. Therefore, only the stiffness matrices for IV, V, VI and IV', V', VI' need be calculated. These will yield the forces at 0 due to displacements at the points 0, 1, 4, 5, 6, and 8. If the force is known (Neumann condition) the displacement at point 0 may be calculated.

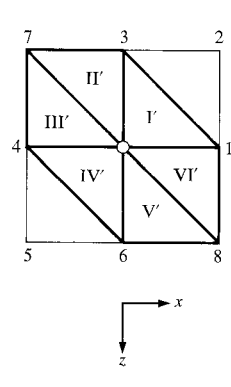
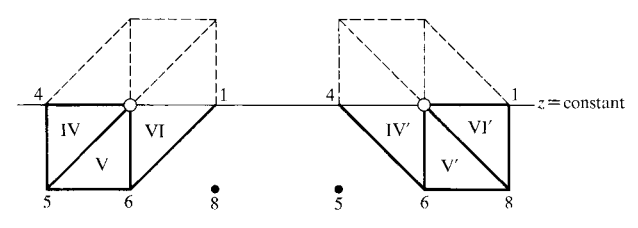


Figure 2 Reflection in the z axis of the tent function of Fig. 1.

Figure 3 The tent functions of Figs. 1 and 2 centered about boundary points lying on a line z = constant. Since the top three surfaces of the tents are outside of the boundary they make no contribution to the stiffness matrix.



Time-dependent problems

The finite element method has been used mainly for static problems, but not exclusively. The usual method for handling a time dependency is to treat the time-dependent term as an additional nodal force. The same procedure is applied to vibration problems. The acceleration term is treated as an inertial force applied at the nodes. The motion is considered harmonic so that the time derivative can be replaced by the angular frequency squared times the displacement, and finally eigenfunctions are obtained.

Treating the time-dependent term as an additional nodal force is equivalent to assuming that the displacement of a node as a function of time is piecewise linear between the sampled time points. This mode of displacement can be demonstrated from the principle of conservation of energy. Let the vector consisting of the applied force acting at each node be designated by \mathbf{F} . The work done by \mathbf{F} over a time interval Δt is

$$\int_{t_0}^{t_0+\Delta t} \mathbf{F}[\boldsymbol{\delta}(t) - \boldsymbol{\delta}(t_0)] dt = \mathbf{F}_{\text{mean}}[\boldsymbol{\delta}(t_0 + \Delta t) - \boldsymbol{\delta}(t_0)], (8)$$

where δ is the displacement vector. From our assumption of piecewise linearity $\mathbf{F}_{\text{mean}} = \mathbf{F}(t_0 + \Delta t/2)$, hence the energy put into the system is

$$\mathbf{F}(t_0 + \Delta t/2) \left[\delta(t_0 + \Delta t) - \delta(t_0) \right]. \tag{9}$$

Similarly, the work done by the stress is

Average Stress · [strain
$$(t_0 + \Delta t)$$
 - strain (t_0)]
= Stress $(t_0 + \Delta t/2) \cdot B[\delta(t_0 + \Delta t) - \delta(t_0)]$
= $B^T D B \delta(t_0 + \Delta t/2) [\delta(t_0 + \Delta t) - \delta(t_0)]$. (10)

The change in kinetic energy is

$$1/2 m[v^{2}(t_{0} + \Delta t) - v^{2}(t_{0})]$$

$$= 1/2 m[\mathbf{v}(t_{0} + \Delta t) - \mathbf{v}(t_{0})][\mathbf{v}(t_{0} + \Delta t) + \mathbf{v}(t_{0})]$$

$$= m \dot{\mathbf{v}}(t_{0} + \Delta t/2)[\boldsymbol{\delta}(t_{0} + \Delta t) - \boldsymbol{\delta}(t_{0})], \qquad (11)$$

where \mathbf{v} and $\dot{\mathbf{v}}$ are the velocity and acceleration vectors, respectively, and m is a diagonal tensor giving the mass associated with each nodal point. Hence

$$\mathbf{F}(t_0 + \Delta t/2) = B^T D B \, \, \delta(t_0 + \Delta t/2) + m \, \, \dot{\mathbf{v}}(t_0 + \Delta t/2) \, \, . \tag{12}$$

If, in addition, the discontinuity in slope in our piecewise linear functions at the sampled time points is slight, then (12) may be applied over two time intervals, and using standard centered difference formulae we find that

$$\delta(t_0 + 2\Delta t) = -\frac{\Delta t^2}{m} \left[B^T D B \ \delta(t_0 + \Delta t) \right]$$

$$+ 2\delta(t_0 + \Delta t) - \delta(t_0)$$

$$+ \frac{\Delta t^2}{m} \mathbf{F}(t_0 + \Delta t) .$$
(13)

Expression (13) is in a form suitable for an explicit iterative solution with all boundary conditions contained in the stiffness matrix, the mass tensor and the force terms.

Propagation of Rayleigh wave on quarter space

As an illustration we will consider the propagation of a Rayleigh wave around a corner. This is an example of a problem possessing a boundary point, the corner, where one previously did not have a difference formula for the free surface, a Neumann condition. A related problem, an interior pulse source located at a point on the interior diagonal, has been treated numerically [6] by the device of rounding off the corner. A Rayleigh wave [7] is an elastic surface wave with both compressional and shear components which has large amplitudes at the surface that decay exponentially with depth. For homogeneous media the expressions in the second section for plane strain will apply.

Figure 4 illustrates the boundary conditions applied at the corner. The known amplitude distributions for the two components of Rayleigh wave motion are applied at each time step on side 1 multiplied by sinusoidal functions varying with time. The phases of the sinusoidal variations applied to the horizontal and vertical displacements are appropriate for a Rayleigh wave propagating

along side 2 from left to right. Vertical displacements are displacements in the z direction. Sides 2 and 3 are treated as free surfaces, stress = 0. The boundary conditions are obtained by calculating the forces at the surface points as a function of the displacements at neighboring points and setting them equal to the inertial force. This yields a relation between the displacement at the boundary point at time $t = t_0 + 2\Delta t$ and $t = t_0$ and the displacements at neighboring points at time $t = t_0 + \Delta t$. In Fig. 4, $\tau = 2\pi/\omega$, the period of the wave.

In expression (13) the value of the mass assigned to each point is also required. For interior points the mass is just ρhk , where ρ is the density, which is assumed constant throughout. Since the integral of a tent function over the plane is just hk, it is a suitable weighting function for calculating m. If we assume ρ constant in a triangular element, the contribution of the element to the mass assigned a point is $1/6 \rho hk$. Therefore points on the boundary which have only three triangles associated with them are assigned a mass of $1/2 \rho hk$.

The relations for points on boundary 2 are calculated to be

$$-2\rho\ddot{u}_{0} = (4\mu/k^{2})(u_{0} - u_{6}) + [(\lambda + 2\mu)/h^{2}](4u_{0} - 2u_{1} - 2u_{4}) + [(\lambda - \mu)/kh](w_{1} - w_{4}) + [(\lambda + u)/kh](w_{5} - w_{8});$$

$$-2\rho\ddot{w}_{0} = (\mu/h^{2})(4w_{0} - 2w_{1} - 2w_{4}) + [4(\lambda + 2\mu)/k^{2}](w_{0} - w_{6}) + [(\lambda - \mu)/kh](u_{4} - u_{1}) + [(\lambda + u)/kh](u_{5} - u_{9}).$$

$$(14)$$

Here double dots indicate second derivatives with respect to time. The relations for points on boundary 3 can be obtained from (14) by suitable transformations. The relations obtained for the right-hand corner point are (see Fig. 5):

$$\begin{aligned} -4\rho\ddot{u}_{0} &= 9\left(\mu/k^{2}\right)\left(u_{0}-u_{6}\right) + 9\left[\left(\lambda+2\mu\right)/h^{2}\right]\left(u_{0}-u_{4}\right) \\ &+ 3\left[\left(\lambda+\mu\right)/kh\right]\left(w_{5}-2w_{0}\right) \\ &+ 3\left(\lambda/kh\right)\left(2w_{6}-w_{4}\right) + 3\left(\mu/kh\right)\left(2w_{4}-w_{6}\right); \\ -4\rho\ddot{w}_{0} &= 9\left(\mu/h^{2}\right)\left(w_{0}-w_{4}\right) \\ &+ 9\left[\left(\lambda+2\mu\right)/k^{2}\right]\left(w_{0}-w_{6}\right) \\ &+ 3\left[\left(\lambda+\mu\right)/kh\right]\left(u_{5}-2u_{0}\right) \\ &+ 3\left(\lambda/kh\right)\left(2u_{4}-u_{6}\right) + 3\left(\mu/kh\right)\left(2u_{6}-u_{4}\right). \end{aligned}$$

The boundary condition on side 4 is a radiation condition. The functional dependence of a Rayleigh wave traveling down side 3 is $A(x)e^{(\omega t - kz)}$ where $k = \omega/c_R$ with ω the angular frequency and c_R the Rayleigh wave phase

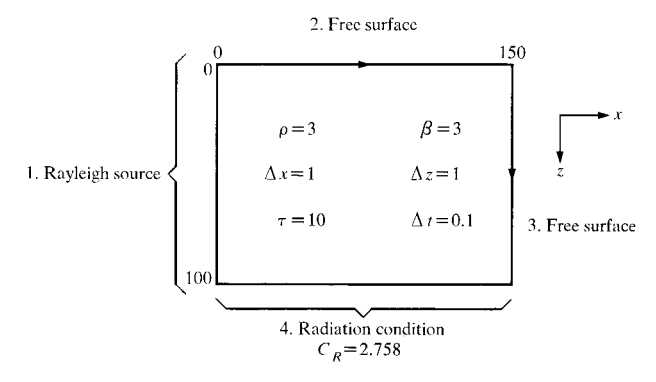
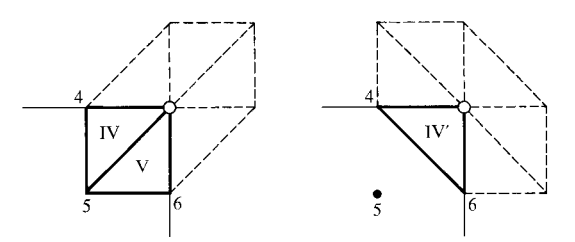


Figure 4 The numerical model used to calculate the transmission of Rayleigh waves around a corner. The boundary conditions shown on the four sides are described in the text.

Figure 5 The tent functions of Figs. 1 and 2 centered about a corner point. Only the elements 1V and V of Fig. 1 contribute to the stiffness matrix and only element IV' of Fig. 2.



velocity. Taking partial derivatives with respect to z and t yields

$$\frac{\partial}{\partial z} \left(\frac{u}{w} \right) + \frac{1}{C_{ij}} \frac{\partial}{\partial t} \left(\frac{u}{w} \right) = 0. \tag{16}$$

This is the equation of the characteristic for outgoing waves with phase velocity $c_{\rm R}$. The difference form of (16) together with (13) suffice to determine the boundary values on side 4 such that no Rayleigh waves are reflected back.

Figure 6 shows various stages of propagation of the Rayleigh wave on the surface of the quarter space. The leading edge of the Rayleigh wave is tapered with a cosine taper to prevent ringing. Table 3 compares the results of this numerical model experiment for the transmission coefficient, T, and phase shift with results from laboratory model experiments. The agreement is good.

Acknowledgments

The numerous matrix multiplications required for this paper were performed with the aid of SCRATCHPAD [11], a symbolic manipulation program for the IBM System 360 Model 67 developed by R. Jenks, F. Blair and J. Griesmer at the IBM Thomas J. Watson Research Center.

369

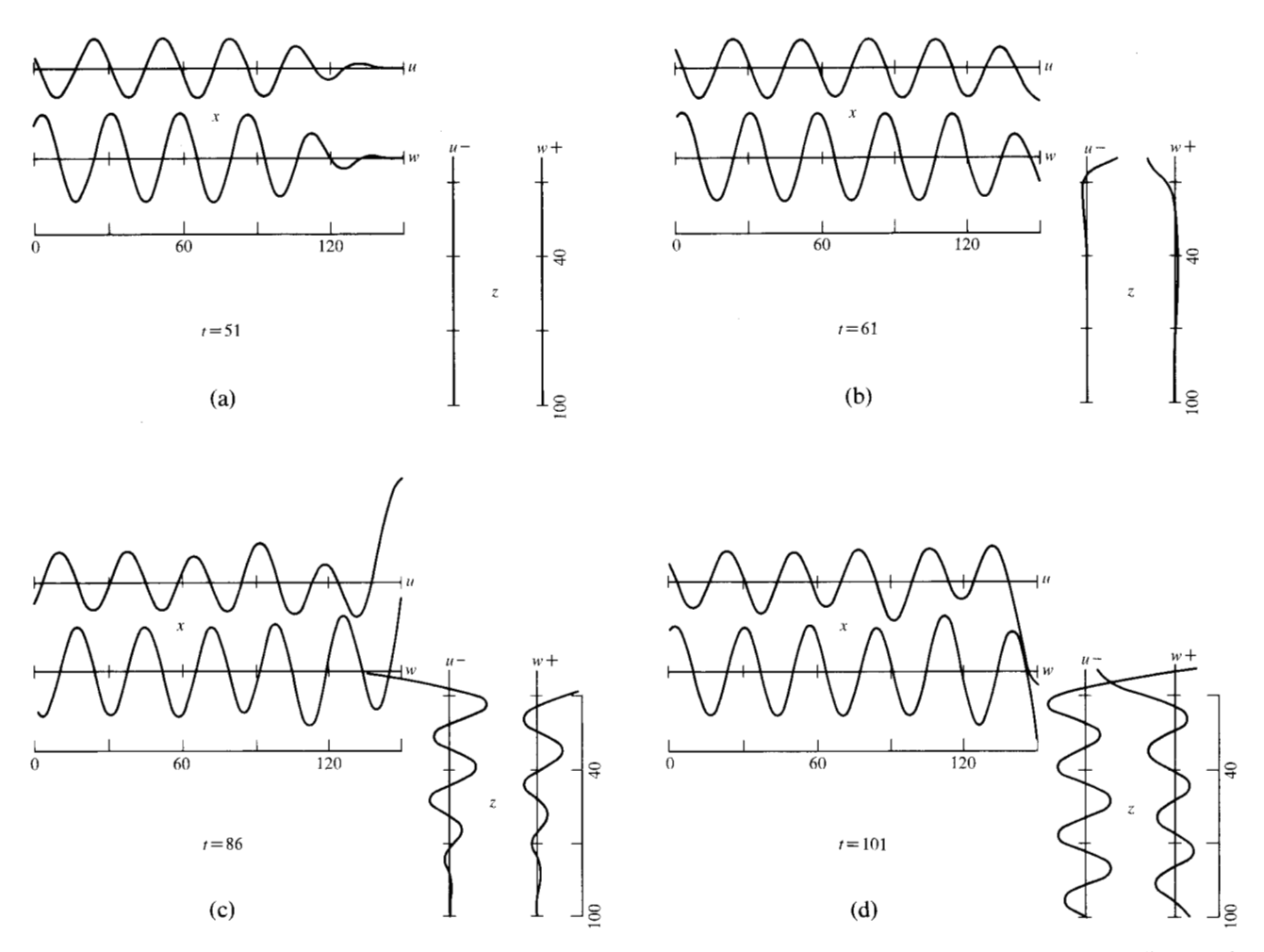


Figure 6 In (a) the leading edge of the tapered Rayleigh wave has reached the corner. The next figure (b) occurs at a time difference of one period from (a). Displacement is now occurring on the right-hand boundary past the corner. In the next figure (c) the leading edge of the tapered Rayleigh wave has reached the bottom boundary where the radiation condition is applied. Sinusoidal motion occurs in u and w on the right-hand boundary with appropriate phase difference at some distance from the corner. The last figure (d) shows the Rayleigh waves propagating about the corner and beyond the bottom boundary. The motions on the top boundary are modulated by a Rayleigh wave reflected from the corner.

Table 3 Transmission of Rayleigh wave around a corner.

	Researchers							
	De Bremaecker [8]	Knopoff and Gangi [9]	Pilant, Knopoff and Schwab [10]	Alsop and Goodman present results				
Physical constants	Polystyrene sheet $\alpha = 1.82$ $\beta = 1.15$ $\sigma = 0.17$	Aluminum sheet $\alpha = 5.76$ $\beta = 3.26$ $\sigma = 0.266$	Aluminum sheet $\alpha = 5.40$ $\beta = 3.12$ $\sigma = 0.25$	Finite element method simulation $\alpha = 5.196$ $\beta = 3.00$ $\sigma = 0.25$ $\rho = 3.00$ DT = 0.05 DX = DZ = 0.5				
T, amplitude	0.633	0.73	0.67	0.645				
Phase shift, degrees	-90	_	-74.9	−83.6 ± 6.5				

References

- 1. M. J. Turner, R. W. Clough, H. C. Martin, and L. J. Topp, "Stiffness and deflection analysis of complex structures," J. Aero. Sci. 23, 805 (1956).
- 2. K. O. Friedrichs and H. B. Keller, "A Finite Difference Scheme for Generalized Neumann Problems," Numerical Solutions of Partial Differential Equations, Academic Press, New York, 1966, p. 1.
- 3. O. C. Zienkiewicz, The Finite Element Method in Structural and Continuum Mechanics, McGraw-Hill Publishing Co., Inc., London, 1967.
- 4. E. R. Lapwood, "The Transmission of a Rayleigh Pulse around a Corner," *Geophysical Journal* 4, 174 196 (1961).
- 5. I. S. Sokolnikoff, Mathematical Theory of Elasticity, Mc-Graw-Hill Publishing Co., Inc., New York, 1946.
- 6. Z. S. Alterman and A. Rotenberg, "Seismic Waves in a Quarter Space," Bull. Seismological Soc. Am. 59, 347 - 368
- 7. W. M. Ewing, W. S. Jardetzky, and F. Press, Elastic Waves in Layered Media, McGraw-Hill Publishing Co., Inc., New York, 1957.

- 8. J. Cl. De Bremaecker, "Transmission and Reflection of
- Rayleigh Waves at Corners." *Geophysics* 23, 253 (1958).

 9. L. Knopoff and A. F. Gangi, "Transmission and Reflection of Rayleigh Waves by Wedges," Geophysics 25, 1203 (1960).
- 10. W. L. Pilant, L. Knopoff, and F. Schwab, "Transmission and Reflection of Surface Waves at a Corner. Pt. 3. Rayleigh Waves (Experimental)," J. Geophys. Res. 69, 291 (1964).
- 11. J. H. Griesmer and R. J. Jenks, "SCRATCHPAD-1: An Interactive Facility for Symbolic Mathematics, Proceedings of the Second Symposium on Symbolic and Algebraic Manipulation, S. R. Petrick, Ed., ACM, March, 1971.

Received November 1, 1972

The authors are located at the IBM Thomas J. Watson Research Center, Yorktown Heights, New York 10598.